Performance Analysis of MIMO Radar with Widely and Closely Separated Antennas

Raed S. M. Daraghma

Department of Electrical and Electronics Engineering
Palestine Technical University, Palestine
Email: R.daraghmeh@ptuk.edu.ps

Abstract— **In this paper, we address the problem of Direction of Departure (DOD) and Direction of Arrival (DOA) estimation for Multiple Input Multiple Output (MIMO) radar. The presented work studies the effect of Radar Cross Section (RCS), Signal to Noise Ratio (SNR) and speed of targets on the performance of the MIMO radar with widely and closely separated antennas. Since the information on the targets is obtained from the echoes of the transmitted signals, it is straightforward that RCS and speed of targets play an important role in system accuracy. Analysis can be used to find the direction of multiple types of targets such as Capon, Multiple Signal Classification (MUSIC) and parallel factor (PARAFAC). To differentiate the meaning of targets, varying targets of different types, such as bicycle, bird, man, ship and jet have been considered. After defining suitable values for each type of target in 2D space, the performance of each type is discussed by using the MATLAB program. Finally, we present an experimental platform of MIMO radar with Bistatic antennas which has been developed in order to evaluate the performance of the above techniques under more realistic conditions.**

Keywords- MIMO Radar; Target Localization; Parallel Factor (PARAFC); Direction of Arrival; Signal to Noise Ratio (SNR).

I. INTRODUCTION

Radar is an electronic device for detection and localization of the target. It works by transmitting a special type of waveform, and detects the echo signal. Radar can be designed to see through conditions impervious to normal human vision, such as darkness, haze, fog, rain, snow. In addition, radar has the advantage of being able to measure target parameters like range and velocity.

Radar is used for a large range of civilian, military and scientific applications like air surveillance, surface search, tracking and guidance, weather radar, Earth observation.

In [1], the author selected a number of different moving targets: simple and complex targets with different RCS and speeds. From the existing work on the application of Capon, MUSIC and PARAFAC to the localization of different targets, he noticed the importance of the types of targets and the effect of changing the speed of targets.

This paper focuses on comparing the performance criterion for different types of targets as well as the impact of the number of antennas on the performance of three different techniques mentioned above.

The radar system can be classified into monostatic and bistatic. The transmitter and receiver of the monostatic radar are located in the same location, while the transmitter and receiver of the biostatic radar are far apart relative to the wavelength used in the radar. According to the characteristics of the transmitted signals the radar system can be further classified into continuous wave for radar and pulse radar. The continuous waveform radar transmits a single continuous waveform while the pulse radar transmits multiple short pulses. Most of the modern radars are monostatic pulse radars [2]. Recently, a new field of radar research called Multiple Input Multiple Output (MIMO) radar has been developed, which can be thought as a generalization of the multi-static radar concept. MIMO radar has multiple transmit and multiple receive antennas as its name indicates [3].

In [4], the transmit and receive antennas may be in the form of an array and the transmit and receive arrays can be co-located or widely separated like phased array systems. Although some types of MIMO radar systems look likes phased array systems, there is a fundamental difference between MIMO radar and phased array radar. The difference is that MIMO radar always transmits multiple probing signals, via its transmit antennas, that may be correlated or uncorrelated with each other, whereas phased array radars transmit scaled versions of a single waveform which are fully correlated. The multiple transmit and receive antennas of a MIMO radar system may also be widely separated as radar networks. The fundamental difference between a multi-static radar network and MIMO radar is that independent radars that form the network perform a significant amount of local processing and there exists a central processing unit that fuses the outcomes of central processing in a reasonable way. For example, every radar makes detection decisions locally then the central processing unit fuses the local detection decisions. Whereas MIMO radar uses all of the available data and jointly processes signals received at multiple receivers to make a single decision about the existence of the target. The key ideas of MIMO radar concept has been picked up from MIMO communications. MIMO is a technique used in communications to increase data throughput and link range without additional bandwidth or transmit power. This is achieved by higher spectral efficiency and link reliability or diversity. Using MIMO systems in communications made significant improvements when there is serious fading in the communication channel. Radar systems also suffer from fading when there are complex and extended targets. Researchers took the idea of using multiple transmit and receive antennas to reduce the effects of fading from communications and applied it in the field of radar to achieve performance enhancements. Some of the most important radar applications are the detection performance

2018, © Copyright by authors, Published under agreement with IARIA - www.iaria.org

and high resolution of the moving target localization. Radar Cross Section (RCS), range, location and velocity are utility parameters of the moving target [5][6]. In [7] and [8], to improve the accuracy of target detection and estimation, antenna arrays have been used. MIMO radar uses multiple transmitter and multiple receiver elements. Generally, unlike the phased-array systems, MIMO radar has several advantages compared to the conventional phased array systems: higher resolution, more degrees of freedom, improved parameter specification, better spatial coverage and detection diversity gain. MIMO radars can be classified into two categories: (1) MIMO radar with widely separated antennas scheme and (2) MIMO radar using collocated antennas, which is similar to phase array radar. In the literature, there are many configurations of MIMO radar according to the location of the transmitting and receiving elements. Widely separated antennas represent one of these configurations. In this scheme, the separation between transmitter and receiver should be large enough to receive the uncorrelated echoes from the different targets. The main advantage of this scheme is that the spatial diversity of the targets RCS enhances the radar performance.

In [9], a bistatic MIMO radar technique with transmission spatial diversity is proposed, and the estimation performance is analyzed. Moreover, the angles with respect to receiver can be determined using the proposed technique. In addition, the maximum number of targets that can be identified with this technique is discussed in this paper. In [10], MIMO radar can deal with multiple targets. Linearly independent waveforms are transmitted at the same time via multiple antennas. These independent waveforms are linearly combined at the targets with different phases, after which the signal waveforms reflected from different targets are linearly independent of each other, which allow for the application of Capon, MUSIC and PARAFAC algorithms.

In this work, we focus on the application of MIMO radar to the estimation of DOA and the DOD of multiple targets exist in the same range bin for bistatic MIMO radar system. We are particularly interested to optimize the average angular error for different types of targets.

The paper is organized as follows: in Section II, the previous work on the subject is summarized. The MIMO radar signal model is presented in Sections III and IV. The performance of MIMO radar is evaluated through simulations via MATLAB in Section V. Some concluding remarks are given in Section IV.

II. RELATED WORK

In [11], the author reviews some recent work on MIMO radar with widely separated antennas, widely separated transmit/ receive antennas capture the spatial diversity of the target's radar cross section (RCS). Unique features of MIMO radar are explained and illustrated by examples. It is shown that with no coherent processing, a target's RCS spatial variations can be exploited to obtain a diversity gain for target detection and for estimation of various parameters, such as angle of arrival and Doppler. For target location, it is shown that coherent processing can provide a resolution for exceeding that supported by the radar's waveform.

In [12], the authors discussed the velocity estimation performance for multiple input multiple output (MIMO) radar with widely spaced antennas. He derived the Cramer-Rao bound (CRB) for velocity estimation and he discussed the optimized configuration design based on CRB. General results were presented for an extended target with reflectively varying with look angle. Also, the analysis was provided for a simplified case, assuming an isotopic scattered. For given transmitted signals, optimal antenna placement was analyzed in the sense of minimizing the CRB of the velocity estimation error. The authors shown that when all antennas are located at approximately the same distance from the target, symmetrical placement is optimal and relative position of transmitters and receivers can be arbitrary under the orthogonal received signal assumption.

In [13], the authors presented compressive sensing in the spatial domain to achieve target localization, specifically direction of arrival (DOA), using multiple input multiple- output (MIMO) radar. A sparse localization framework was proposed for MIMO array in which transmit and receive elements are placed at random. This allows for dramatic reduction in the number of elements needed, while still attaining performance comparable to that of a filled (Nyquist) array. The authors developed a bound on the coherence of the resulting measurement matrix, and obtained conditions under which the measurement matrix satisfies the so-called isotropy property. The coherence and isotropy concepts are used to establish uniform and non-uniform recovery guarantees within the proposed spatial compressive sensing framework. In the proposed framework, compressive sensing recovery algorithms are capable of better performance than classical methods, such as beamforming and MUSIC.

There are many existing methods to localize the moving target. The Angle of Arrival (AOA), the Angle of Departure (AOD), the speed of the target, and the RCS are the most used parameters to localize a moving target. In [10], the author proposed a Capon technique. In [14], the author proposed a MUSIC (Multiple Signal Classification) technique. In [15], the author proposed parallel factor analysis (PARFAC).

In this paper, we compare between three well-known techniques (Capon, MUSIC and PARFAC) by selecting a number of different moving targets: simple and complex targets with different RCS and speeds. Moreover, two cases of localizations are taken: widely and closely separated MIMO radar antennas. The performance of the three different techniques were noticed and the impact of the number of antennas are discussed.

III. MIMO RADAR SIGNAL MODEL

Let us consider a bistatic MIMO radar of M_t transmit and M_r receive antennas. If $X_i(n)$ is the baseband signal transmitted

2018, © Copyright by authors, Published under agreement with IARIA - www.iaria.org

from antenna at frequency $f_c = c/\lambda_c$, the signal received by a target located at an angle θ_t in the far field is:

$$R(m,\theta_t) = a_T^t(\theta_t)X(n) \quad (1)$$
$$n = 1, 2, \ldots\ldots\ldots N$$

Where N denotes the total number of symbols transmitted from each antenna, $X(n)$ is the vector of transmitted symbols at time index n.

$$X(n) = [X_1(n), X_2(n), \ldots X_T(n)] \quad (2)$$

and $a_T(\theta)$ is the transmit steering vector which take into account the relative delay at each antenna

$$a_T(\theta) = \left[e^{j\frac{2\pi}{\lambda_c}T_1(\theta)}, e^{j\frac{2\pi}{\lambda_c}2(\theta)}, \ldots, e^{j\frac{2\pi}{\lambda_c}T_n(\theta)}\right] \quad (3)$$

Using equation (1), the transmitted power at specific direction θ is defined as

$$P(\theta) = E\{a_T^T(\theta)\, x(n) x^H(n) a_T^*(\theta)\} = a_T^T(\theta)\, R\, a_T^*(\theta) \quad (4)$$

R is the covariance matrix of the transmitted waveforms. If the waveforms are orthogonal, i.e., $R = I_{nT}$, the power is equally transmitted in all directions and adaptive detection techniques can be applied without the need for scanning.

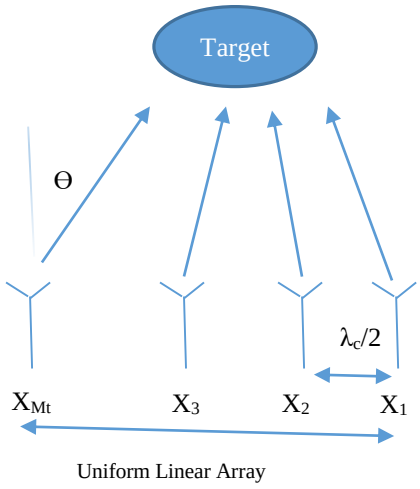

Figure 1. Diagram of a Uniform Linear Array Radar.

If a Uniform Linear Array (ULA) radar with half-wavelength inter-element spacing is considered (see Fig. 1), the expression of the excess distance $d_i(\theta)$ traveled by the signal transmitted from antenna i becomes

$$d_i(\theta) = (i-1)\frac{\lambda_c}{2}\sin(\theta) \quad (5)$$

and the expression of the steering vector a_T becomes

$$a_T(\theta) = \left[1 \quad e^{j\,2\pi\sin(\theta)} \ldots e^{j\,(n_r-1)\pi\sin(\theta)}\right] \quad (6)$$

Assuming that the target has a reflection coefficient β_t and moves with a radial velocity V_r, it produces a normalized Doppler shift f_{dt} such that

$$f_{dt} = \frac{V_r}{c} f_c \quad (7)$$

By defining the receive steering vector a_R as

$$a_R(\theta) = \left[1 \quad e^{j\,2\pi\sin(\theta)} \ldots e^{j\,(n_R-1)\pi\sin(\theta)}\right] \quad (8)$$

the reflected echo from the target are denoted by

$$Y_i(n) = \beta_t\, e^{j2\pi n f_{dt}}\, a_R^T(\theta)\, x(n) \quad (9)$$

Moreover, let L be the number of static interferers located at the angles θ_1 to θ_L and with reflection coefficients β_1 to β_L. In the presence of a centered white Gaussian noise w, the received signals after matched filter can be expressed in a vector form as

$$Y(n) = \beta_t\, e^{j2\pi n f_{dt}}\, a_R^T(\theta)\, x(n) + \sum_{i=1}^{L} \beta_t a_R(\theta_i)\, a_T^T(\theta_i)\, x(n) + w(n)^2 \quad (10)$$
$$n = 1, 2, \ldots\ldots\ldots N$$

To take advantage of the virtual array concept, the inter-element spacing of the transmit antenna should be M_t times higher than the inter-element spacing at the receiver (see Fig. 2).

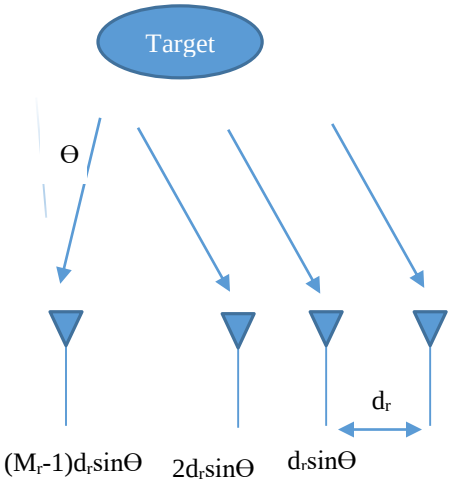

Figure 2. Radar with multiple receive antennas.

In this section, we consider that the Coherent Processing Interval (CPI) consists of Q consecutive pulse periods. The Swerlling II target model as in [16] was assumed, where RCS

2018, © Copyright by authors, Published under agreement with IARIA - www.iaria.org

coefficient is varying from pulse to pulse. The targets are located in the far-field. The RCS coefficients are assumed to vary independently from pulse to pulse, and the propagation medium is non dispersive.

The baseband received signal at the output of the receive array after synchronization can be written as:

$$X_q = B(\emptyset) \sum_q A^T(\theta) S + W_q \quad (11)$$

$$q = 1, 2, .. Q$$

$X_q \in R^{M_r \times L}$ collects the L samples received by M_r antennas for the q^{th} pulse period. $\sum_q diag(C_q)$, with $c_q = [\delta_{1q}, \ldots \delta_{kq}]$ $\delta_{kq} = \alpha_{kq} e^{j(q-1)x}$, i.e., x_q is the Doppler frequency of the k^{th} target [9]. The RCS coefficients δ_{kq}, $k = 1, \ldots K$, are varying independently from pulse to pulse, and $W_q \in R^{M_r \times L}$ is the noise interference term. MIMO radar transmits mutually orthogonal waveforms. We assume that $1/SLS^H = I_M$. After right multiplication of (11) by $(1/L)\, S * S^H$, the matched filter output is:

$$Y_q = B(\emptyset) \sum_q A^T(\theta) + Z_q \quad (12)$$
$$q = 1, 2, .. Q$$

$$Y_q = \frac{1}{LXS^H} \epsilon Ç M_r \times M_t^2 \quad , \quad Z_q = \frac{1}{LWS^H}$$

Let us factorize (12):

$$Y_q = (A(\varphi) \odot B(\theta) C_q^T + Z_q \quad (13)$$
$$Y_q = \text{vec}(Y_q), \; Z_q = \text{vec}(Z_q)$$

which can be written in the compact form:

$$Y = (A(\varphi) \odot B(\theta) C^T + Z \quad (14)$$

$Y = [Y_q, \ldots, Y_Q]$ and $Z = [Z_q, \ldots, Z_Q]$ are of size $M_t M_r \times Q$ and $C^T = [C_1^T, \ldots, C_Q^T]$ is of size $K \times Q$.

In [17], the Capon estimator can be written as:

$$P(\varphi, \theta) = \frac{1}{a(\varphi) \odot b(\theta)^H R_{YY}^{-1} (a(\varphi) \odot b(\theta)} \quad (15)$$

where $R_{yy} = \left(1/Q\right) Y Y^H$

The MUSIC estimator can be written as:

$$P_{MUSIC}(\varphi, \theta) = \frac{1}{a(\varphi) \odot b(\theta) E_Y E_Y^H (a(\varphi) \odot b(\theta)} \quad (16)$$

$E_y = M_t M_r \times (M_t M_r - k)$ is the matrix contains the noise eigenvectors of R_{yy}. In [18], the third Estimator PARAFAC was derived. PARAFAC implies the transmit and receive angles relative to the same target are automatically paired.

IV. DATA MODEL

In this section, we consider the multiple pulses, multiple arrays case. The MIMO radar system has the following parameters:

- transmit array M_t .
- receive array M_r .
- K targets in a far field.
- Q transmitted pulses, and the RCS is varying independently from pulse to pulse.
- δ_{kq} is the reflection coefficient of the k^{th} target during the q^{th} pulse.
- $\{\theta\}_{k=1}^K$, $\{\varphi\}_{k=1}^K$ are the DODs and DOAs with respect to transmit and receive array, respectively.
- $A(\theta) = [a(\theta_1), \ldots, a(\theta_k)]$ is the transmit steering vector relative to K targets, $B(\varphi) = [b(\varphi_1), \ldots, b(\varphi_k)]$ is receiving steering, vector relative to K targets.

V. SIMULATION RESULTS

In this section, MATLAB program simulation results are presented to verify the above analysis and compare the performance of the three techniques (Capon, MUSIC and PARAFAC). Bistatic radar (see Fig. 3) and Localization of the multiple targets for a Uniform Linear Array (ULA) configuration at the transmitter and receiver can be achieved by the algorithms [15].

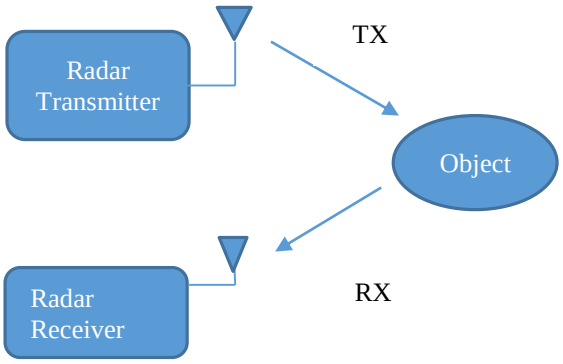

Figure. 3. Schematic of a bistatic radar design

We generate the matrices S, A and B as explained in the previous section $[S]_m$ is generated by:

$$[S]_m = (1 + j/2)[H_N]_m \quad (17)$$

H_N is the $N \times N$ Hadamard matrix, and N is fixed to 256. The Signal to Noise Ratio (SNR) at the receiver is defined as:

$$SNR = 10 \log\left(\sum_{q=1}^{Q} |B \sum_q A^T S| F / |W|^2 \; F\right) \quad (18)$$

2018, © Copyright by authors, Published under agreement with IARIA - www.iaria.org

where Additive White Gaussian Noise (AWGN) is assumed, and $\|.\|_F$ is the Frobenis norm. We consider ULA transmit and receive arrays with $\lambda/2$ inter-element spacing for both arrays. For the Swerlling II target model, each column of the matrix $C \in R^{Q \times k}$ is generated from a complex Gaussian distribution with zero mean and variance $\sigma^2_{\delta k}$.
The Doppler X_k is generated by:

$$X_k = \frac{2\pi V_k \ T_p}{\lambda} \quad (19)$$

V_k is the target velocity, $T_p = 5 \times 10^{-6}$ is the pulse duration in seconds, $\lambda = 3 \times 10^8 / f_c$ with $f_c = 1\ GHz$.

This subsection analyzes the impact of the number of targets on the performance detection. The performance criterion is the absolute value of the difference between the true angle and estimated angle, averaged over transmit and receive angles and over all targets.

In a first experiment (Fig. 4), we consider seven types of targets. The variance and speed of each target was given in Table I. We simulate the presence of two to six targets, starting from K = 2 with DODs = $[10^\circ, 20^\circ]$ and DOAs = $[0^\circ, 30^\circ]$ until K = 6, DODs = $[10^\circ, 20^\circ, 30^\circ, 40^\circ, 50^\circ, 60^\circ]$ and DOAs = $[0^\circ, 30^\circ, 5^\circ, 15^\circ, 25^\circ, 30^\circ]$. The number of pulses is Q = 100, number of samples for each transmitted pulses is L = 512, SNR =10 dB, and Swerlling II model is chosen. We plotted the performance of the Capon method, and we compared the performance of the different types of targets via Monte Carlo simulation.

From Fig. 4, it is clear that a better angular resolution is achieved when the target is "Man" and the worst angular resolution is achieved when the target is "Car". From Fig. 4, we observe that the global performance of all types of targets seriously degrade when the number of targets is increased.

In Fig. 5, we simulate the presence of two to six targets. The other parameters are the same as in Fig. 4, but, in this case we have plotted the performance of the MUSIC technique. We compare the performance of the different types of targets via Monte Carlo simulation. From Fig. 5, it is clear that a better angular resolution is achieved when the target is "Boat" and the worst angular resolution is achieved when the target is "Fighter". From Fig. 5, we observe that the global performance of all types of targets seriously degrades when the number of targets is increased. In Fig. 6, we simulate the presence of two to six targets. The other parameters are the same as in Fig. 4, but, in this case, we have plotted the performance of the parallel factor (PARAFC) technique, and we compared the performance of the different types of targets via Monte Carlo simulation.

From Fig. 6, it is clear that the best angular resolution is achieved when the target is "Car" and the worst angular resolution is achieved when the target is "Jet". From Fig. 6, we observe that the global performance of all types of targets seriously degrades when the number of targets is increased.

Table I. RCS AND SPEED FOR DIFFERENT TYPES OF TARGETS

Target Type	Radar cross section fot target (m^2)	Speed of target (m/s^2)
Bicycle	2	10
Man	1	6.5
Car	100	100
Fighter	40	125
Boat	0.02	20
Jumbo Jet	100	40
Bird	0.01	150

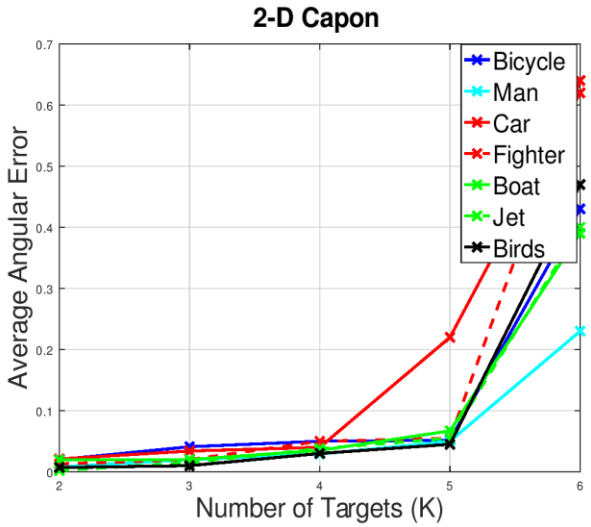

Figure 4. Average angular error with number of targets (2-D Capon case)

This subsection analyzes the impact of signal to noise ratio on the performance detection. In a second experiment, we simulate the presence of three targets (K = 3) characterized by DODs = $[10^\circ, 20^\circ, 30^\circ]$ and DOAs = $[-10^\circ, -20^\circ, 0^\circ]$. The number of pulses Q = 100, the number of samples for each transmitted pulse

2018, © Copyright by authors, Published under agreement with IARIA - www.iaria.org

L = 512, the number of transmit and receive sub arrays is fixed to 5, SNR $\in (0, 2, 4, 6, 8, 10)$ dB, and the Swerling II model is chosen. We plotted the performance of the Capon method, and we compared the performance of the different types of targets via Monte Carlo simulation.

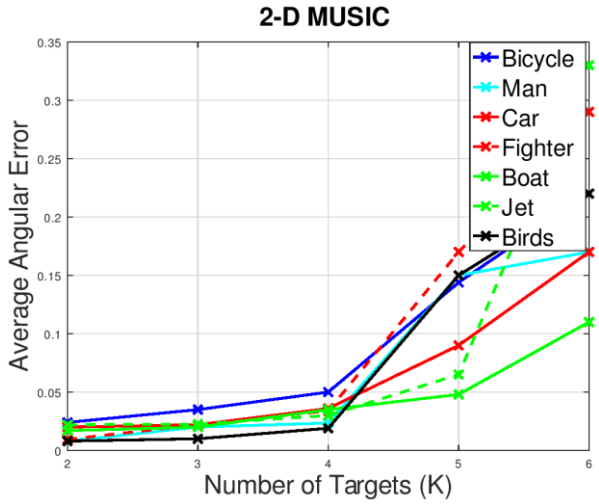

Figure 5. Average angular error with number of targets(2-D MUSIC case)

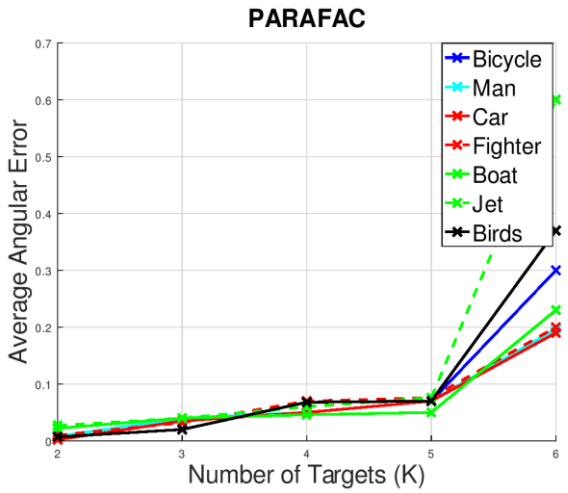

Figure 6. Average angular error with number of targets (PARAFAC case)

From Fig. 7, it is clear that the best angular resolution is achieved when the target is "Bird" and the worst angular resolution is achieved when the target is "Bicycle". As expected, from Fig. 7, we observe that the performance of all types of targets improves when the signal to noise ratio increases. In Fig. 8, we simulate the presence of three targets. The other parameters are the same as in Fig. 4, but, in this case, we have plotted the performance of the MUSIC technique, and we compared the performance of the different types of targets via Monte Carlo simulation. From Fig. 8, it is clear that a better angular resolution is achieved when the target is "Bird" and the worst angular resolution is achieved when the target is "Bicycle".

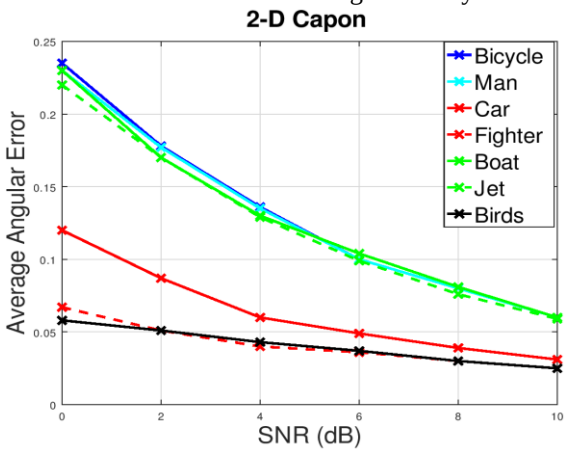

Figure 7. Average angular error with signal to noise ratio for each target (2-D Capon case)

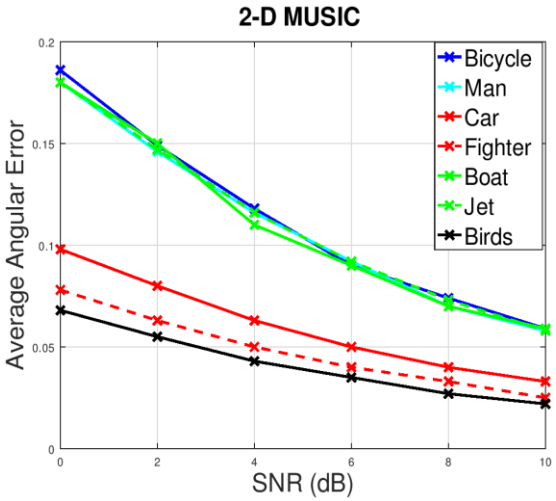

Figure 8. Average angular error with signal to noise ratio for each target (2-D MUSIC case)

In Fig. 9, we simulate the presence of three targets. The other parameters are the same as in Fig. 7, but, in this case, we have plotted the performance of the parallel factor (PARAFAC) technique and we compared the performance of the different types of targets via Monte Carlo simulation. From Fig. 9, it is clear that the best angular resolution is achieved when the target is "Bird" and the worst angular resolution is achieved when the target is "Jet".

Case 1: performance of the seven target for closed spaced, SNR = 0 dB.

In Fig. 10, we plot the true angles for the seven targets (K = 7) for closely spaced (θ, φ) Car = $(-80, 70)$, bicycle =

2018, © Copyright by authors, Published under agreement with IARIA - www.iaria.org

$(-75, 65)$, man = $(-40, 50)$, fighter = $(-35, 45)$, boat = $(0, -10)$, jumbo jet = $(5, -15)$, bird = $(15, -5)$. The other parameters are: the speeds and RCS for each target as shown in Table I, the number of pulses Q = 100, the number of samples for each transmitted pulse L = 512, the number of transmit and receive sub arrays is fixed to 8, SNR = 0 dB, and the Swerlling II model is chosen. In Figs. 11-13, we compare the performance of different localization techniques via Monte Carlo simulations.

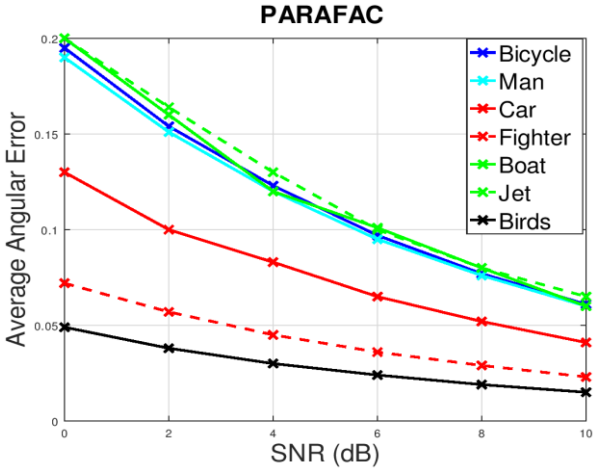

Figure 9. Average angular error with signal to noise ratio for each target (PARAFAC case)

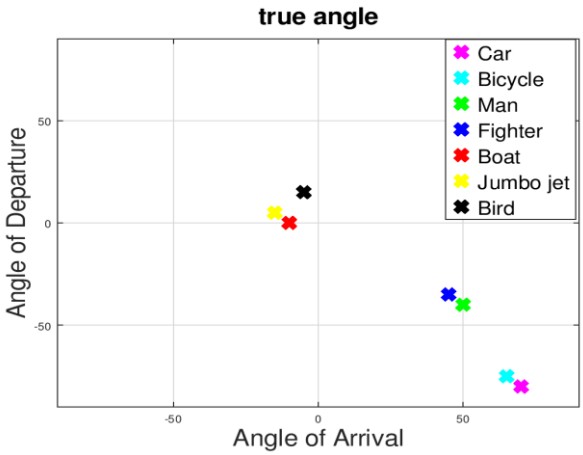

Figure 10. True angles for the targets

In Figs. 11- 13, we have plotted the 2-way Capon, 2-way music and PARFAC. For the comparison between all methods to be fair, the angular resolution of the two latter techniques is fixed to 0.0001 degree.

Case 2. performance of the seven target for closed spaced, SNR = 30 dB

In Fig. 11, we can see from seven targets, 2-way Capon technique can detect 3 targets which are: car, boat and bird respectively, the average angular error is 57.1 degree.
From Fig. 12, we can also see that the 2-way music technique can detect 3 targets from seven which are: car, man and bird respectively, the average angular error is 57.2 degree.

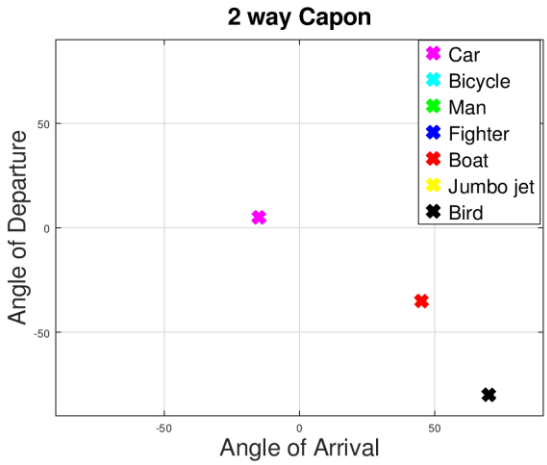

Figure 11. Localization of the seven closely spaced targets by using 2-way Capon technique (SNR = 0 dB).

In Fig. 12, we can see that the PARAFC technique can detect 6 targets from seven which are all the targets except car target, the average angular error is 5. 6 degrees. From these results we can conclude that none of the above techniques can be detected all the targets, because we need to change some parameters, i.e., the angles of arrival and departure (widely spaced or closely spaced), the other parameter is signal to noise ratio. The other conclusion is the superiority of PARFAC among the other techniques.

We plot the true angles for the seven targets for closely spaced (θ, φ) Car = $(-80, 70)$, bicycle = $(-75, 65)$, man = $(-40, 50)$, fighter = $(-35, 45)$, boat = $(0, -10)$, jumbo jet = $(5, -15)$, bird = $(15, -5)$. The other parameters are: the speeds and RCS for each target as shown in table 1. The number of pulses Q = 100, the number of samples for each transmitted pulse L = 512, the number of transmit and receive sub arrays is fixed to 8, SNR = 30 dB, and the Swerlling II model is chosen.
From the comparison between Figs. 14 and 16, it is clear that a better detection and angular resolution (regardless of the technique used) is achieved when the signal to noise ratio increases from 0 to 30 dB. For instance, six targets were detected in 2-way Capon technique (car, man, jumbo jet, bird, fighter and boat), five targets were detected in 2-way music technique (car, man, boat, bird and jumbo jet), and all targets were detected in PARAFAC technique.

2018, © Copyright by authors, Published under agreement with IARIA - www.iaria.org

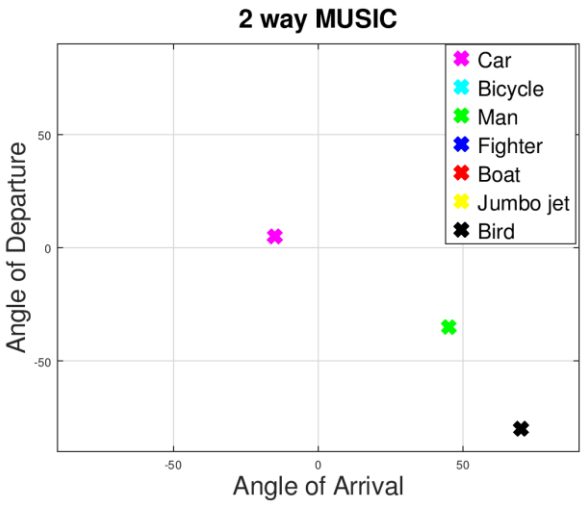

Figure 12. Localization of the seven closely spaced targets by using 2-way Music technique (SNR = 0 dB).

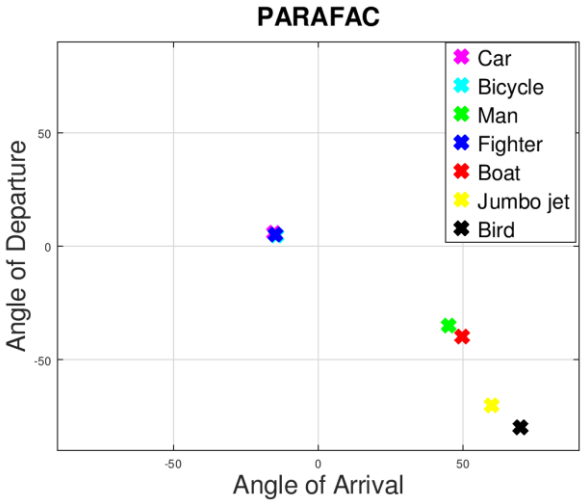

Figure 13. Localization of the seven closely spaced targets by using PARAFAC technique (SNR = 0 dB).

In this section, we illustrate the performance of estimator via Monte Carlo simulation consisting of 100 runs for each value of the SNR. Number of pulses is fixed to 100, 512 samples per pulse and the number of targets to K = 4 for closely spaced $(\theta, \varphi) = (-80, 70), (-75, 65), (-40, 50), (-35, 45)$. The RCS coefficient of the car is $(100\, m^2)$, and the speed of target is $100\ \mathrm{m/s^2}$. Fig. 17 shows the evolution of the error for the cases $M_t = M_r$, with either 3 to 7 antennas. Fig. 17 shows that increasing the number of transmit and receive arrays from 3 to 7 improves the global performance. Fig. 15 shows the evolution of the error for the cases $M_t = M_r$, with either 3 to 7 antennas. Fig. 18 shows that increasing the number of transmit and receive arrays from 3 to 7 improves the global performance. From the comparison between Figs. 17 and 18, it is clear that a better angular resolution is achieved when the targets are widely spaced.

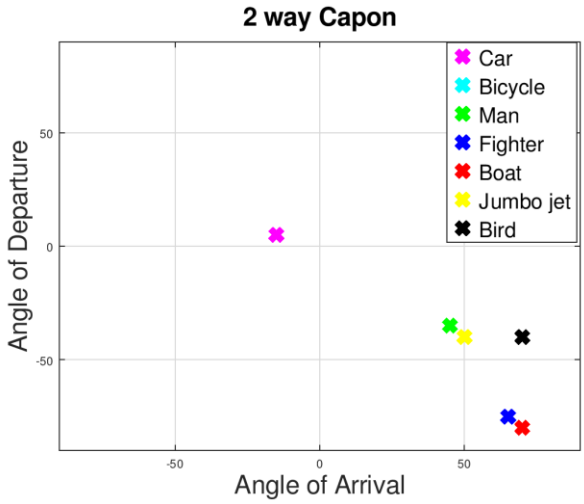

Figure 14. Localization of the seven closely spaced targets by using 2-way Capon technique (SNR = 30 dB).

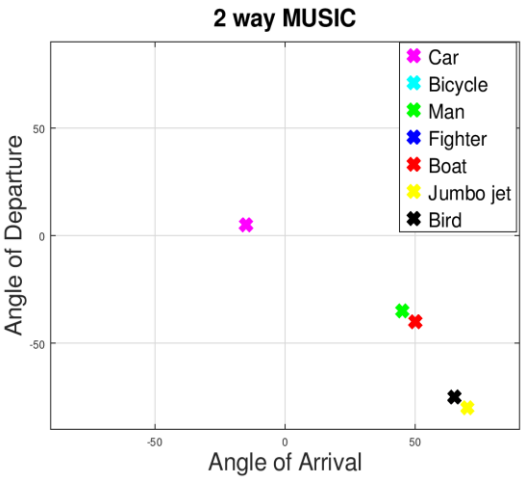

Figure 15. Localization of the seven closely spaced targets by using 2-way Music technique (SNR = 30 dB).

In this section, we illustrate the performance of estimator via Monte Carlo simulation consisting of 100 runs for each value of the SNR. Number of pulses is fixed to 100, 512 samples per pulse and the number of targets to K = 4 for widely spaced $(\theta, \varphi) = (-80, 70), (-40, 10), (0, 50), (40, -30)$. The RCS coefficient of the car is $(100\, m^2)$, and the speed of target is $100\ \mathrm{m/s^2}$.

In Fig. 19, we have plotted the two-way MUSIC spectrum, for K = 5 targets with DODs = $[40^\circ, 35^\circ, 30^\circ, 40^\circ, 65^\circ]$ and DOAs = $[20^\circ, 25^\circ, 30^\circ, 50^\circ, -45^\circ]$, i.e., for the three closely spaced targets and two targets widely spaced from the others. The number of pulses is Q = 100, number of samples for each

2018, © Copyright by authors, Published under agreement with IARIA - www.iaria.org

transmitted pulses is L = 512, SNR =10 dB, and Swerlling II model is chosen. With $M_t = 4$ transmit and $M_r = 4$ receive antennas. Two-way MUSIC does not allow accurate localization of the three closely spaced targets, since one cannot clearly distinguish three peaks in the spectra, while the two other targets well localized.

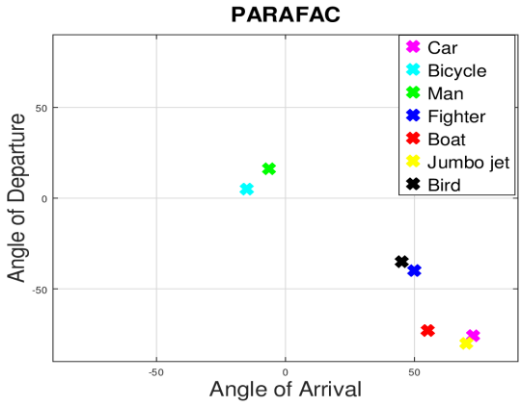

Figure 16. Localization of the seven closely spaced targets by using PARAFAC technique (SNR = 30 dB).

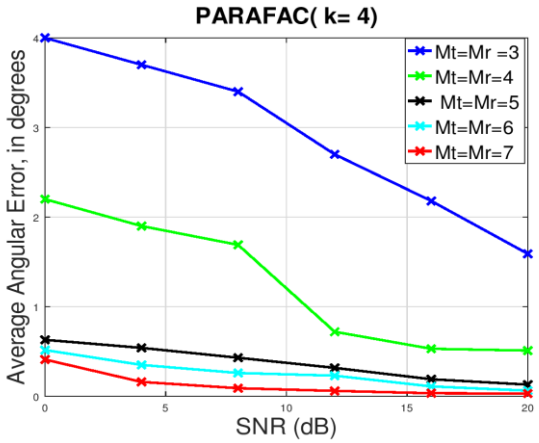

Figure 17. Signal to noise ratio verses the average angular error (closely spaced)

In Fig. 20, we have plotted the two-way MUSIC spectrum, for K = 5 targets with DODs = $[40^{\circ}, 35^{\circ}, 30^{\circ}, -40^{\circ}, 65^{\circ}]$, and DOAs =$[20^{\circ}, 25^{\circ}, 30^{\circ}, 50^{\circ}, -45^{\circ}]$, i.e., for the three closely spaced targets and two targets widely spaced from the others. The number of pulses is Q = 100, number of samples for each transmitted pulses is L = 512, SNR =10 dB, and Swerlling II model is chosen. With $M_t = 10$ transmit and $M_r = 10$ receive antennas. In this case, the spatial resolution significantly improves when the number of transmit and receive antennas increases from 4 to 10, the three closely spaced targets now become distinguishable.

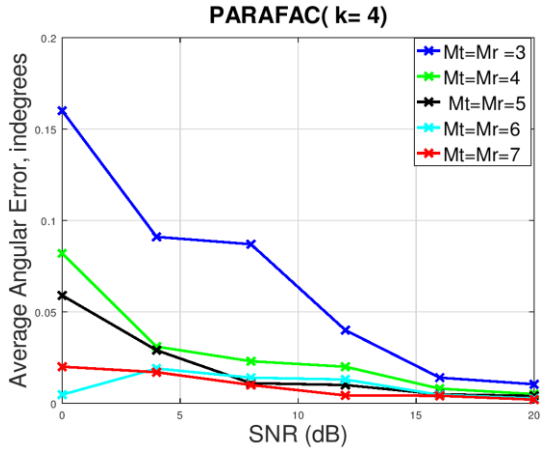

Figure 18. Signal to noise ratio verses the average angular error (widely spaced).

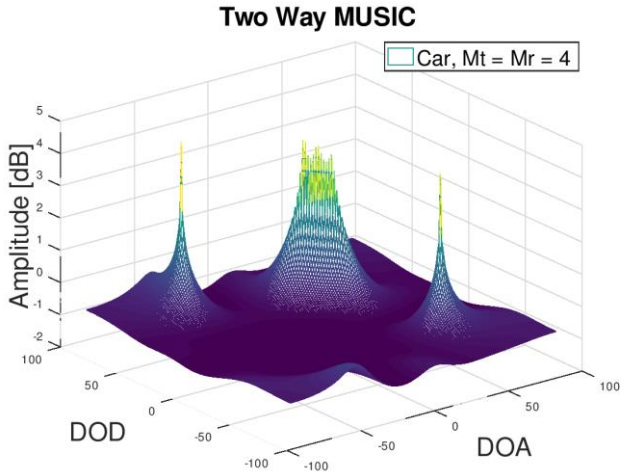

Figure 19. Two-way MUSIC spectrum for $M_t = M_r = 4$, K = 5 targets.

VI. CONCLUSION

In this paper, we have considered the detection and localization of moving target in bistatic MIMO radar with widely separated antennas, where multiple antennas transmit linearly independent waveforms and multiple antenna receive the reflected signal. We can significantly improve the estimation accuracy of the bistatic MIMO radar techniques as well as enhance their performance. The main problems encountered in MIMO radar detection are radar cross section and speed of the target. To illustrate the impact of these two parameters on the performance of MIMO radar, several types of targets and three popular techniques (Capon, MUSIC and PARAFC) were

2018, © Copyright by authors, Published under agreement with IARIA - www.iaria.org

considered for comparison. From the simulation results, we have shown that irrespective of the radar cross section and speed of target a high performance (low angular error) can be obtained when the signal to noise ratio increases. On the contrary, low performance can be obtained when the number of targets increases.

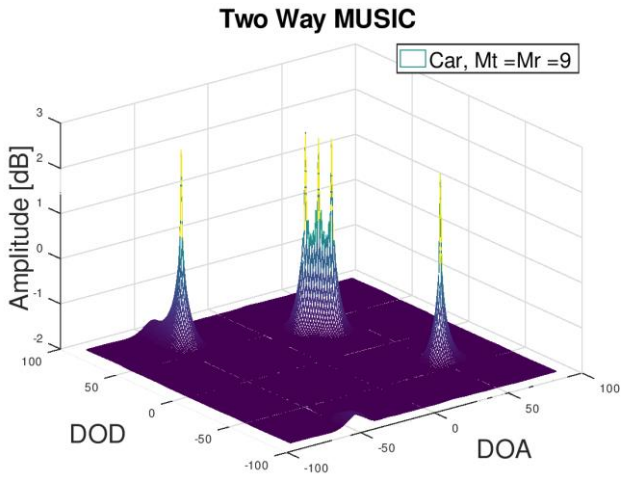

Figure 20. Two-way MUSIC spectrum for $M_T = M_r$ = 10, K = 5 targets.

REFERENCES

[1] R. S. Daraghma, "The Effect of Radar Cross Section and Speed of Target on the Detection of MIMO Radar," SPACOMM 2018, The Tenth International Confernce on Advances in Satellite and Space Communications, pp. 38-42.

[2] M. A. Richards, Fundamentals of Radar Signal Processing, McGraw-Hill, 2005.

[3] J. Li, P. Stoica, "MIMO Radar Signal Processing," Wiley, 2009

[4] E. Fishler, A. Haimovich, R. Blum, L. J. Cimini, D. Chizhik, and R. Valenzuela, "Spatial Diversity in Radars – Models and Detection Performance," IEEE Transactions on Signal Processing, vol. 54, no. 3, pp. 823-838, Mar. 2006.

[5] G. R. Curry, Radar System Performance Modeling, 2nd ed. Norwood, MA; Artech House, 2005.

[6] M. I. Skolnik, Introduction to Radar Systems, 3rd ed. New York; McGraw-Hill, 2001.

[7] D. W. Bliss and K. W. Forsythe, "Multiple-input multiple-output (MIMO) radar and imaging: degrees of freedom and resolution," in Proc. of the 37th Asilomar Conference. Signals, Systems, and Computer, Pacific Grove, CA, Nov. 2003, vol. 1, pp. 4-59.

[8] F. C. R obey, S. Coutts, D. Weikle, J. C. McHarg, and K. Cuomo, "MIMO radar theory and experimental results," in Proc. Thirt-Eighth Asilomar Conference. Signals, Systems, and Computer, 7-10 Nov. 2004, Pacific Grove, CA, USA, vol. 1, pp. 300-304.

[9] E. Fishleret al, "MIMO radar: an idea whose time has come," in Proceedings of the IEEE Radar Conference, pp. 71-78, Philadelphia, Pa, USA, April 2004.

[10] J. Capo, "High-resolution frequency- wave number spectrum analysis," Proceedings of the IEEE, 57(8): 1408 { 1418, 1969. doi:10.1109/PROC. 1969.7278}.

[11] A. Haimovich, R . Blum, and L. Cimini, "MIMO Radar with Widely Separated Antenna," IEEE Signal Processing Magazine, pp. 116-129, January 2016.

[12] Q. He, R. Blum, H. Godrich, A. Haimovic, "Target Velocity Estimation and Antenna Placement for MIMO Radar with Widely Separated Antennas," IEEE Journal of Selected Topics in Signal Processing, pp. 79-100, vol. 4, no. 1, February 2010.

[13] M. Rossi, A. Haimovich, Y. Eldar, "Spatial Compressive Sensing for MIMO Radar," IEEE Transaction on Signal Processing, vol. 62, no. 2, pp. 419-430, January 2014.

[14] R. O. Schmidt, "Multiple emitter location and signal parameter estimation," IEEE Transactions on Antennas and Propagation, ISSN 0018-926X, 34(3), pp. 276-280.

[15] A. Cichocki, D. Mandic, A-H. Phan, C. Caiafa, G. Zhou, Q. Zhao, and L. De Lathauwer, "Tensor decompositions for signal Processing applications from two-way to multiway component analysis," arXiv: 1403.4462, DOI: 10.1109/MSP. 2013.2297439. vol. 32, pp. 145-463, 2014

[16] C. Y. Chen and P.P. Vaidyanathan, "MIMO radar space-time adaptive processing using prolate spheroid wave function," IEEE Transaction on Signal Processing, vol. 56, no. 2, pp. 623-635.

[17] H. Yan, J. Li, and G. Liao, "Multitarget identification and localization using bistatic MIMO radar systems," EURASIP J. Adv. In Signal Process. pp. 77-78, 2008.

[18] D. Nion and N. D. Sidiropoulos, "A PARAFAC- based technique for detection and localization of multiple targets in a MIMO radar system," in Proc. IEEE Int. Conf. Acoust., Speech Signal Process. (ICASSP). pp. 2077-2080, 2009.

2018, © Copyright by authors, Published under agreement with IARIA - www.iaria.org